Liquid Crystals
Publication details, including instructions for authors and subscription information:
http://www.informaworld.com/smpp/title~content=t713926090

Switching behaviour and electro-optic response due to the soft mode ferroelectric effect in chiral smectic A liquid crystals

I. Abdulhalim[a]; G. Moddel[a]
[a] Department of Electrical and Computer Engineering and Optoelectronic Computing Systems Center, University of Colorado, Boulder, Colorado, U.S.A.

To cite this Article Abdulhalim, I. and Moddel, G.(1991) 'Switching behaviour and electro-optic response due to the soft mode ferroelectric effect in chiral smectic A liquid crystals', Liquid Crystals, 9: 4, 493 — 518
To link to this Article: DOI: 10.1080/02678299108033148
URL: http://dx.doi.org/10.1080/02678299108033148

LIQUID CRYSTALS, 1991, VOL. 9, NO. 4, 493–518

Switching behaviour and electro-optic response due to the soft mode ferroelectric effect in chiral smectic A liquid crystals

by I. ABDULHALIM and G. MODDEL*

Department of Electrical and Computer Engineering and Optoelectronic Computing Systems Center, University of Colorado, Boulder, Colorado 80309-0425, U.S.A.

(*Received 6 August 1990; accepted 1 November 1990*)

The switching characteristics and the electro-optic response due to the electroclinic effect in chiral smectic A liquid crystals are analysed theoretically. We give an exact analytic solution to the dynamic equation of the tilt angle (θ) up to the θ^4 term in the Landau expansion of the free energy. The non-linear behaviour of θ and the characteristic time under an applied electric field are described near the $S_A^* \rightarrow S_C^*$ transition. They both have a finite value at the transition which depends on the field. The characteristic time (τ_θ) exhibits a critical slowing down at sufficiently low fields, which occurs only in the early stages of the switching. At late stages, the switching time exhibits a maximum at a particular temperature which depends on the field, and then decreases in a very narrow temperature range near the transition. The θ^4 term is important in explaining certain properties even for very small θ, and it becomes essential for $\theta > 5°$. The optical response of an electroclinic liquid crystal cell is considered in detail. We derive an expression for the output intensity of light passing through an electroclinic cell. The delay and rise times for the optical signal are shown to a first approximation to be $0{\cdot}379\,\tau_\theta$ and $2{\cdot}577\,\tau_\theta$, respectively.

1. Introduction

The soft mode ferroelectric (electroclinic) effect in chiral smectic A (S_A^*) liquid crystalline mesophase was first described and observed by Garoff and Meyer [1, 2]. Based on a symmetry argument similar to that for ferroelectricity in the tilted phases of chiral smectic liquid crystals, they predicted the existence of the electroclinic effect. An electric field applied to a chiral, non-tilted smectic liquid crystal may induce an inclination of the molecules in the plane normal to the electric field. Recently considerable attention has been devoted to the electroclinic effect, both from practical and fundamental points of view. The nature of the transition from the S_A^* to chiral smectic C (S_C^*) phase under an applied electric field is still a matter of controversy due to different estimations of the critical exponent for the effective susceptibility which controls the tilt [1–6]. Recently the electroclinic effect was reported for more ordered smectic structures [7, 8] than the S_A^* phases as well as for a chiral nematic liquid crystal [9].

From a practical point of view the electroclinic effect allows for electro-optic switching which is a factor of 10–100 faster than the surface stabilized ferroelectric liquid crystal, depending on the material and the temperature [10]. In addition, the electroclinic effect is continuous with the field and does not show bistability, allowing for grey level applications [11]. Although the electroclinic effect exists in the surface stabilized ferroelectric liquid crystal case, it is a minor effect; that is, the changes in the

* Author for correspondence.

tilt angle θ (soft mode) are negligible compared to the changes in the azimuth angle φ (Goldstone mode), except when very close to the S_C^*–S_A^* transition [12]. For thick enough cells where the helicoidal structure exists in the S_C^* phase it is possible to suppress the Goldstone mode by applying an electric or a magnetic DC field such that the helix is unwound and a homogeneous structure is obtained [13, 14].

The phenomenological treatment of the electroclinic effect thus far has been for very small induced tilt angles and has included only the θ^2 term in the Landau expansion of the free energy [1, 2]. This approximation yields an induced tilt angle which varies linearly with the field and inversely proportional to the temperature. The switching time was shown to be independent of the field and inversely proportional to temperature. For liquid crystal mixtures which exhibit induced tilt angles of less than a few degrees this linear approximation has been verified experimentally to be satisfactory, at least for temperatures far from the transition [12]. With the advent of new electroclinic materials with higher electroclinic coupling constants, a non-linear behaviour of the induced tilt angle and the switching speed have been observed [12–16]. In the present work we solve the dynamic equation of motion for θ analytically up to the θ^4 term in the Landau expansion. We explain the non-linear behaviour near the transition, and reveal other new properties which await experimental verification. In § 2 the geometry and formulation of the problem are given. In § 3 the analytic solutions are derived and simplified approximate expressions for several cases are given. In § 4 the behaviour is presented graphically and discussed. In § 5 we characterize the electro-optic response of an electroclinic device, which may be used to analyse the measured electro-optic response.

2. Geometry and formulation

The cell configuration commonly used to observe a large electroclinic effect has the planar geometry shown in figure 1. In this geometry the molecular layers are stacked perpendicular to the top and bottom glass substrates, which are coated with transparent conducting oxide electrodes. In the field-free state the molecular director $\hat{n}$ is along the layers normal $\hat{z}$ lying in the plane of the substrates. Applying an electric field E between the two plates results in a rotation of the director in the plane of the substrates in a direction which depends on the sign of E. Let $E_\pm$ designate the field along $\pm\hat{x}$, respectively, and $\theta=\theta_\pm$ be the respective induced rotations. We consider the case of uniform alignment, i.e. no twist in the x direction exists due to polar interactions [17], and there is no pretilt of the layers. For electro-optic measurements the cell is usually mounted between crossed polarizers, as shown in figure 1, so that the amplitude of the transmitted light is modulated.

Following Garoff and Meyer [1, 2], the Landau description of the bulk elastic free energy per unit area of S_A^* phase can be written as

$$F=F_0+\int\left[\tfrac{1}{2}a'\theta^2+\tfrac{1}{4}b\theta^4+\ldots+\tfrac{1}{2}\chi_p^{-1}P^2-\frac{\varepsilon_0E^2}{8\pi}-PE-c\theta P\right]dx, \tag{1}$$

where F_0 represents contributions to F from the undisturbed S_A^*. P is the component of the average molecular polarization parallel to E, ε_0 is the dielectric constant excluding contributions from the permanent dipole, χ_p is a generalized susceptibility, c is the electroclinic coupling constant between θ and P, and a' and b are the usual Landau-expansion coefficients for second order phase transitions where $a'=a_0'(T-T_0)$, and where a_0' and b are temperature independent and T_0 is the phase transition temperature for the racemic mixture.

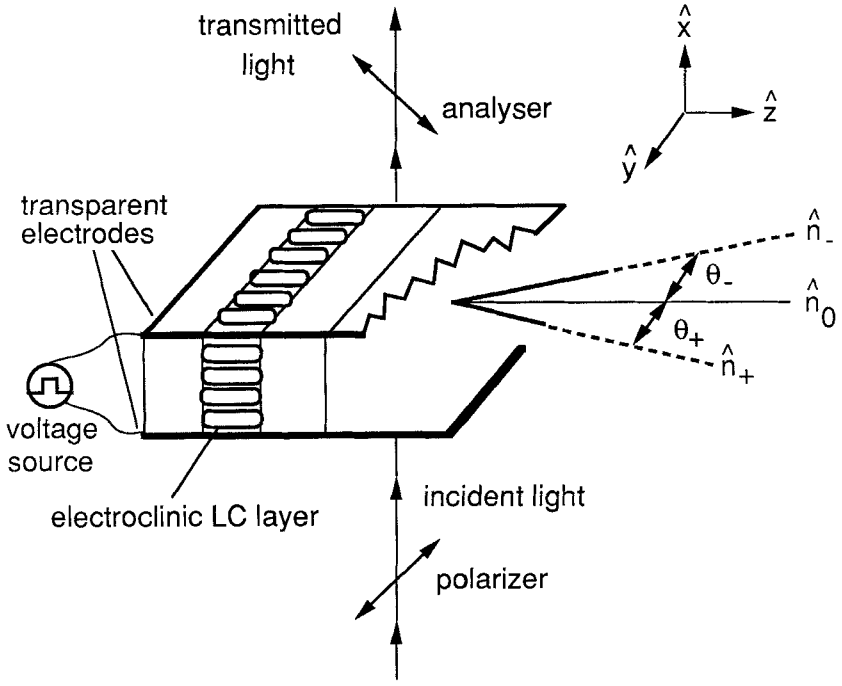

Figure 1. Schematic showing the geometry of the electroclinic liquid crystal structure between the two glass substrates coated with transparent conducing oxide as electrodes.

In [12], Andersson *et al.* included an effective small elastic term in the Landau expansion to account for the interaction with cell walls. This way they were able to describe the switching both in the C* and A* phases, allowing the transition to be smooth. Trajectories to a field were drawn and showed non-vanishing φ in a narrow temperature range over T_c. However, the validity of the included elastic term is not well established. In the present work we take $\varphi = 0$ and consider changes only in θ. We show that this description is adequate to explain many features of the electroclinic switching and allows for analytic solutions.

Since P is an independent variable, its equilibrium value is found by setting $\partial F/\partial P$ to zero, with the result that

$$P = \chi_p(E + c\theta). \tag{2}$$

Inserting (2) into (1), the following form for F is obtained:

$$F = F_c + \int [\tfrac{1}{2}a\theta^2 + \tfrac{1}{4}b\theta^4 + \ldots - c\chi_p\theta E]\, dx. \tag{3}$$

Here F_c includes both F_0 and all the terms which have no dependence on θ and therefore do not contribute to the torque balance equation. The product $c' = c\chi_p$ is the coupling constant between θ and E. The factor a is now the effective susceptibility controlling the tilt of the director near the S_A^*–S_C^* transition, and is given by $a = a' - c^2\chi_p$. The shift from a' to a by $c^2\chi_p$ indicates a renormalization of the transition temperature from T_0 for the non-chiral transition. Thus $a = a_0(T - T_c)$ with the temperature independent constant a_0 and T_c is the new transition temperature. It was stated by

Garoff and Meyer [1, 2] that a goes to zero on the S_A^* side of the chiral transition as some power law $a=a_0(T-T_c)^\gamma$. The experimental values obtained for the critical exponent γ are controversial, but they are close to $\gamma\approx 1$ which is more consistent with the mean field description of the S_A^*–S_C^* transition than the XY model [1–6].

The dynamic equation for the motion of θ from equation (3) is given by the Euler–Lagrange equation

$$\eta_\theta \frac{\partial\theta}{\partial t}=c\chi_p E-a\theta-b\theta^3. \tag{4}$$

Here η_θ is the rotational viscosity associated with the θ motion. Since the electroclinic effect depends strongly on temperature, the dependence of η_θ on temperature must be considered. Generally η_θ is assumed to show only a simple Arrhenius form

$$\eta_\theta=\eta_0\exp(E_a/T), \tag{5}$$

where E_a is the activation energy in units of the Boltzmann constant. However, recently [18], there have been indications that η_0 may exhibit a critical behaviour near the A*–C* transition of the form, $\eta_\theta\approx(T-T_c)^{-0.25}$. In § 4 we will show that this cannot be the case.

3. Analytical solutions

The steady-state solution to equation (4) is given by the roots of the algebraic equation

$$c\chi_p E-a\theta-b\theta^3=0. \tag{6}$$

The only real physical solution to this for $a>0$ (Appendix A) is given by

$$\theta_s=U_+ + U_-, \tag{7}$$

where θ_s is the steady-state value of the induced tilt angle, and

$$U_\pm=\left(\frac{c\chi_p E}{2b}[1\pm\sqrt{(1+\zeta)}]\right)^{1/3}, \tag{8}$$

where $\zeta=4a^3/(27bc^2\chi_p^2E^2)$.

3.1. *Response to a step potential*

The exact time-dependent solution to equation (4), with the condition that $\theta=0$ at $t=0$ and that E changes quickly from $E=0$ at $t=0$ to E (step potential), is given by (Appendix A)

$$t=\frac{\eta_\theta[g(0)-g(\theta)]}{(6b\theta_s^2+2a)}, \tag{9}$$

where

$$g(\theta)=\ln\left(\frac{(\theta_s-\theta)^2}{\theta^2+\theta\theta_s+\theta_s^2+(a/b)}\right)-\frac{2\sqrt{3}\theta_s}{U_+-U_-}\arctan\left(\frac{\theta_s+2\theta}{\sqrt{3}(U_+-U_-)}\right). \tag{10}$$

When the θ^4 term in the Landau expansion is neglected, the solution to equation (4) is given by

$$\theta(t)=\theta_0[1-\exp(-t/\tau_0)], \tag{11}$$

where the steady state induced tilt angle is

$$\theta_0 = \frac{c\chi_p E}{a_0(T - T_c)}, \tag{12}$$

and the characteristic time for θ motion is

$$\tau_0 = \frac{\eta_\theta}{a_0(T - T_c)}. \tag{13}$$

Equations (11), (12) and (13) have been useful for the description of the electroclinic switching behaviour in the linear regime where θ_0 is very small [1, 2, 10–12, 15, 16]. When the tilt angle is larger than a few degrees, the θ^4 term becomes important and equations (7)–(10) must be used for a full description of the electroclinic effect. It is evident that there may be large deviations from the linear approximation. To this end, we consider several special cases for equation (7)–(10). When $\zeta \ll 1$, that is close to the transition and for high fields, we show that (Appendix A)

$$\theta_s = \left(\frac{c\chi_p E}{b}\right)^{1/3}. \tag{14}$$

For small fields and far from the transition ($\zeta \gg 1$) one finds that $\theta_s = \theta_0$ (Appendix A). This is expected because in this limit the induced tilt angle is so small that the θ^4 term in negligible and the response is linear (equations (11)–(13)).

To see how the characteristic time for θ motion varies with field qualitatively, we write equation (9) in the form (Appendix A)

$$\theta(t) \approx \theta_s[1 - \exp(-t/\tau_s)], \tag{15}$$

with the time constant

$$\tau_s = \frac{\eta_\theta}{(3b\theta_s^2 + a)}. \tag{16}$$

In the limit where $\zeta \ll 1$ we find

$$\tau_s \approx \frac{\eta_\theta}{(3b^{1/3}(c\chi_p E)^{2/3})}. \tag{17}$$

In the limit where $\zeta \gg 1$, $\tau_s = \tau_0$ as expected.

In the following section we will show that if an approximation is to be considered, then equations (15) and (16) are good approximations for $\theta < 5°$, and in general, are better approximations than the linear approximation equations (11)–(13).

3.2. *Relaxation*

For the relaxation after the field is turned off, which results in a decay of the tilt angle, we need to solve the dynamic equation for $E = 0$ with the initial condition $\theta = \theta_s$ at $t = 0$. The exact solution is given by (Appendix A)

$$\theta(t) = \frac{\theta_s \exp(-t/\tau_0)}{(1 + (b/a)\theta_s^2(1 - \exp(-2t/\tau_0)))^{1/2}}, \tag{18}$$

where τ_0 is defined in equation (13).

When the θ^3 term in equation (4) is neglected, the solution (18) reduces to $\theta \approx \theta_s \exp(-t/\tau_0)$ as expected for the linear response. This is the case for small fields and

temperatures far from T_c. Conversely, there can be large field dependence for the relaxation time near the transition and for strong fields through the dependence of the initial tilt θ_s on the previously applied field. That is, the relaxation time depends on the initial state of the cell because of the non-linear terms. The time required for θ to decay to any fraction $1/v$ of its initial value θ is found from equation (18) to be

$$\tau_{rel}=\frac{\tau_0}{2}\ln\left(\frac{av^2+b\theta_s^2}{a+b\theta_s^2}\right). \tag{19}$$

Whenever the linear approximation is good, $b\theta_s^2\to 0$, τ_{rel} behaves like τ_0.

For the case where the field is strong enough and near the transition, the relaxation time may have a strong field dependence. The temperature dependence of τ_{rel} resembles that of τ_0, however, there is no true divergence at the transition since τ_{rel} drops to zero at this point. These characteristics of the relaxation behaviour demonstrate that the linear approximation is not adequate near the transition. From relations (11)–(13) of the linear regime, the electroclinic response appears to be symmetric with identical characteristic rise and relaxation times independent of the field which should diverge at the transition (critical slowing down). Here we have shown that because of the non-linearity the relaxation is, in fact, not symmetric, particularly near the transition.

3.3. *Bipolar switching*

For bipolar switching we assume the field is E_+ from $t=0$ to $t=t_+$, and that it then switches quickly to E_-. The solution for $0\leqslant t\leqslant t_+$ is given in equation (9), and the solution for $t>t_+$ is given by

$$\frac{6b}{\eta_\theta}\left(\theta_{s-}^2+\frac{a}{3b}\right)t=g(\theta(t_+),\theta_{s+},E_+)-g(\theta,\theta_{s-},E_-)+\frac{6b}{\eta_\theta}\left(\theta_{s+}^2+\frac{a}{3b}\right)t_+, \tag{20}$$

where θ_{s+} and θ_{s-} are the steady state tilt angles which correspond to E_+ and E_-.

For a symmetric squarewave $|E_+|=|E_-|$ we have $\theta_{s+}^2=\theta_{s-}^2=\theta_s^2$ and equation (20) becomes

$$\frac{6b}{\eta_\theta}\left(\theta_s^2+\frac{a}{3b}\right)(t-t_+)=g(\theta(t_+),\theta_{s+},E_+)-g(\theta,\theta_{s-},E_-). \tag{21}$$

Equations (20) and (21) are useful for electroclinic devices since a bipolar field induces twice the optic axis rotation than that of a monopolar field. For the description of the switching behaviour and the device physics it is adequate to take the case of step field, equation (9). Then the bipolar switching case may easily be understood. The relaxation behaviour in equation (18) and (19) is also of interest and is discussed below.

4. Results and discussion

The constants a_0 and b do not vary substantially from one liquid crystal mixture to another. For our simulations we have chosen: $a_0=3{\cdot}0\times10^4\,\mathrm{N/m^2\,K}$ and $b=8{\cdot}5\times10^5\,\mathrm{N/m^2}$. The critical exponent for the susceptibility which controls the tilt has been taken as $\gamma=1$. The values for the electroclinic coupling constant, the generalized susceptibility, and the viscosity have been chosen such that a relatively large molecular rotation is observed. These chosen values, close to those obtained for the BDH mixture M764E are $c\chi_p=7{\cdot}2\times10^{-4}\,\mathrm{F-V/m^2}$ and $\eta_0=5{\cdot}26\times10^{-4}\,\mathrm{N\,s/m^2}$. The temperature dependence of the viscosity is of the Arrhenius form of equation (5) with the activation energy $E_a=2\times10^3$ in units of the Boltzmann constant.

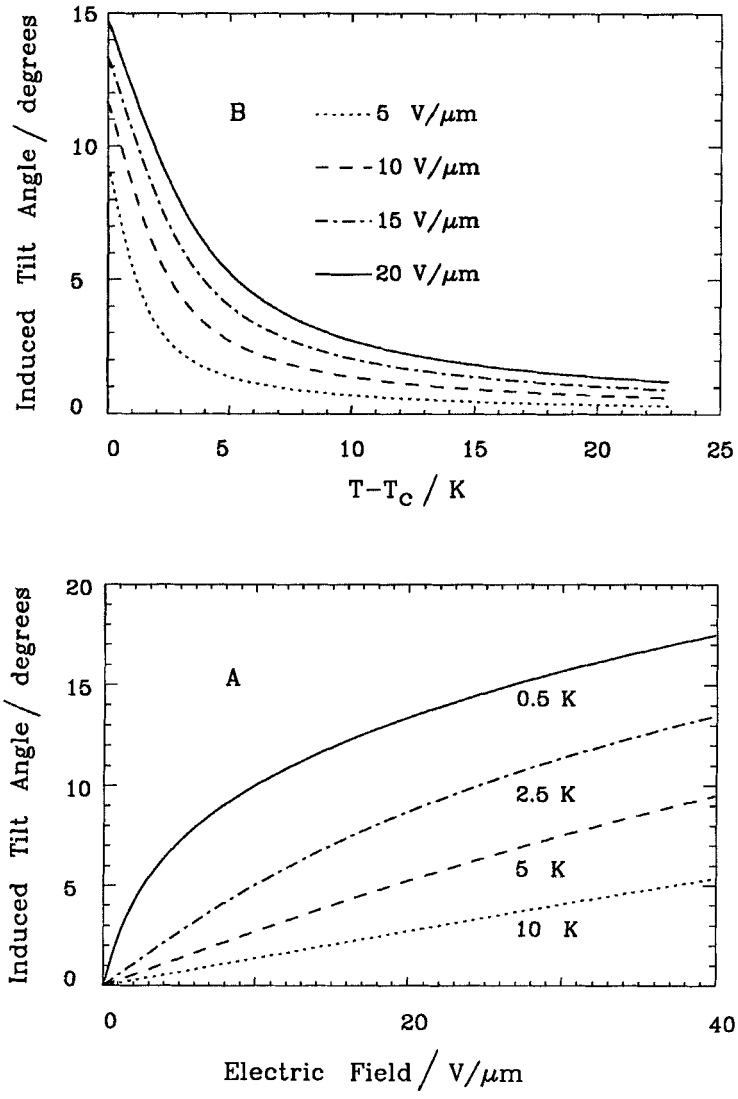

Figure 2. (A) The steady-state induced tilt angle versus the applied electric field at different temperatures, as indicated. (B) The steady-state induced tilt angle versus temperature at different field strengths, as indicated.

4.1. *Static behaviour*

The general behaviour of the induced tilt angle versus electric field and temperature according to equation (7) is shown in figure 2. The linear growth of θ with E is seen to occur only for $\theta < 5°$, that is for small fields and far from the transition temperature T_c. The slope $d\theta/dE$ of the linear part is shown to be enhanced near T_c, while the $E^{1/3}$ saturation behaviour of θ for $\theta > 5°$ occurs for high fields and very close to T_c. The enhancement of $d\theta/dE$ for small fields and near T_c is a pretransitional effect which is expected from the linear regime in equation (12) and has been observed experimentally [1–8] in different liquid crystal materials, including in chiral nematics [9] which exhibit

the electroclinic effect. Here we should mention that $d\theta/dE$ does not diverge at the transition as expected from the linear approximation in equation (12). From equations (7) and (8) it approaches the value $(c\chi_p/27bE^2)^{1/3}$ as $T\to T_c$. The $E^{1/3}$ behaviour of θ, on the other hand, has been observed only for $\theta>5°$, frequently without satisfactory explanation [12, 15, 16]. The decay of θ with $(T-T_c)$ is seen in figure 2 (*b*) as expected also from the linear approximation. As $T\to T_c$ the induced tilt angle has a finite value which depends on the field according to relation (14); from the linear approximation θ is supposed to exhibit divergence, which has never been observed. The inclusion of the θ^4 term in the free energy gives the finite value for θ and $d\theta/dE$ as $T\to T_c$. Measuring these quantities as $T\to T_c$ directly yields the product $c\chi_p$ and its field dependence.

4.2. *Dynamic behaviour*

The temporal evolution of θ at different temperatures and fields is shown in figure 3. From equation (9) the growth is close to but not precisely exponential. In figure 4, $\theta(t)$ is plotted at different $(T-T_c)$ and E using the exact solution in equation (9), the approximate solution in equation (15), and the linear approximation in equation (11). The linear approximation is sufficient in the early stages of switching, since the induced tilt is small. The exponential growth in equation (15) is a good approximation both in the early and late stages, but it is generally a little too high in the intermediate region. The agreement is excellent for temperatures far from T_c. This indicates that equation (15) rather than equation (11) should be used for the case of small tilt angles for an exponential fit.

The characteristic time (τ_θ) for θ motion, defined as the time constant for an exponential growth, is shown in figure 5 as a function of temperature and field. It is seen that τ_θ has no field dependence far from T_c, as expected from the linear regime where the induced tilt is small. The decrease of τ_θ with the field near T_c is due solely to the non-linear θ^3 term in equation (4). This was observed first by Nishiyama *et al.* [15], later by Andersson *et al.* [12], with no explanation. A more detailed experimental study of the field dependence of θ and τ_θ was performed later by Lee and Patel [16]. Their explanation for the non-linear behaviour of τ_θ with E was based on an approximate solution to the dynamic equation (4) and no quantitative comparison was given. When θ is very small, the θ^3 term is negligible compared to the linear term and this decay will be difficult to observe experimentally.

The characteristic time increases as $T\to T_c$. According to the linear approximation τ_θ diverges at the transition and exhibits what is called a critical slowing down, a frequently reported property of the transition. Here we show that critical slowing down occurs only in the early stages of switching. That is, the time interval required to reach approximately $\theta=0{\cdot}8\theta_s$ exhibits a critical slowing down, while for $\theta>0{\cdot}8\theta_s$ the characteristic time exhibits a maximum at a particular temperature close to T_c. It then decreases very close to the transition, reaching a finite value as $T\to T_c$. We observed this maximum in simulations of the time interval required for θ to reach $0{\cdot}96\theta_s$. From our calculations we found that for $\theta\leqslant 0{\cdot}8\theta_s$ there is a critical slowing down and for $\theta\geqslant 0{\cdot}8\theta_s$ there exists the above-described maximum. In figure 6 we show the time interval required for θ to move from $0{\cdot}8\theta_s$ to $0{\cdot}96\theta_s$ showing that during this interval the maximum is quite pronounced. The position of the maximum shifts toward larger $(T-T_c)$ with increasing E, and its magnitude, measured with respect to the value of τ at T_c, becomes smaller. This latter property indicates that the maximum will be observable even more easily at small induced tilt angles than at larger ones. Therefore the late stages of switching cannot be modelled without the non-linear term, even for

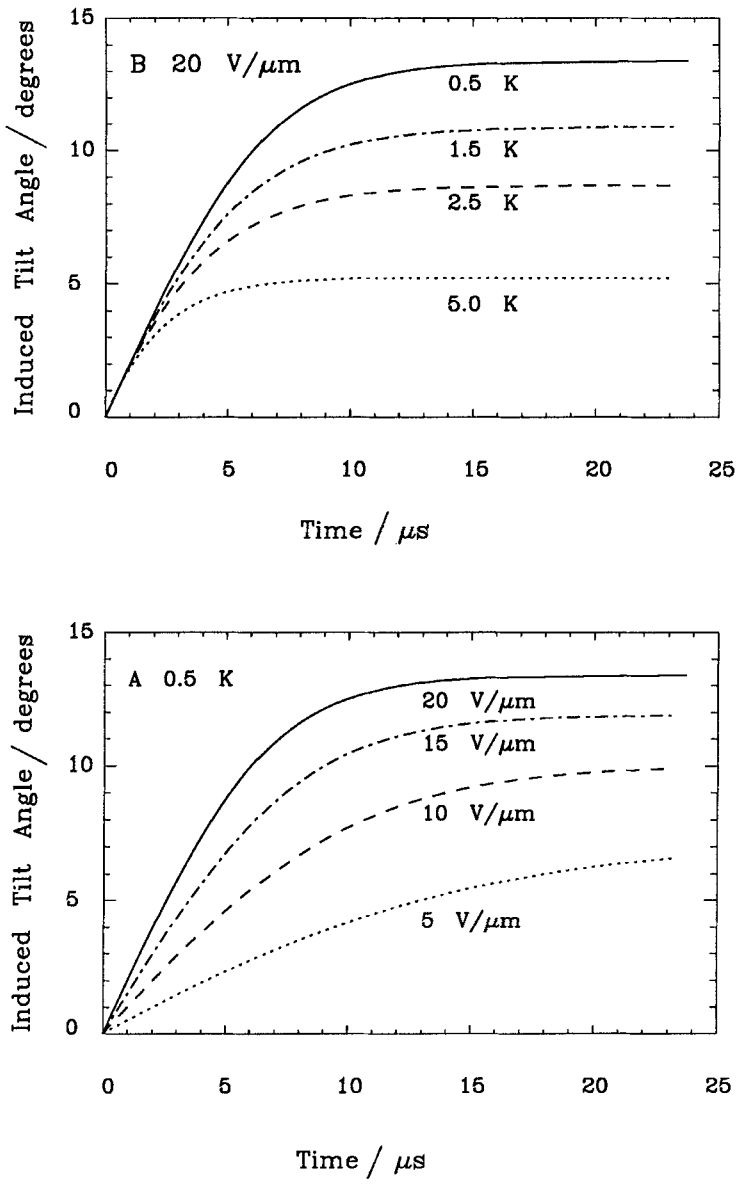

Figure 3. (A) Temporal evolution of the induced tilt angle in response to a step potential at constant temperature and different field strengths, as indicated. (B) Temporal evolution of the induced tilt angle in response to a step potential at constant electric field and various temperatures.

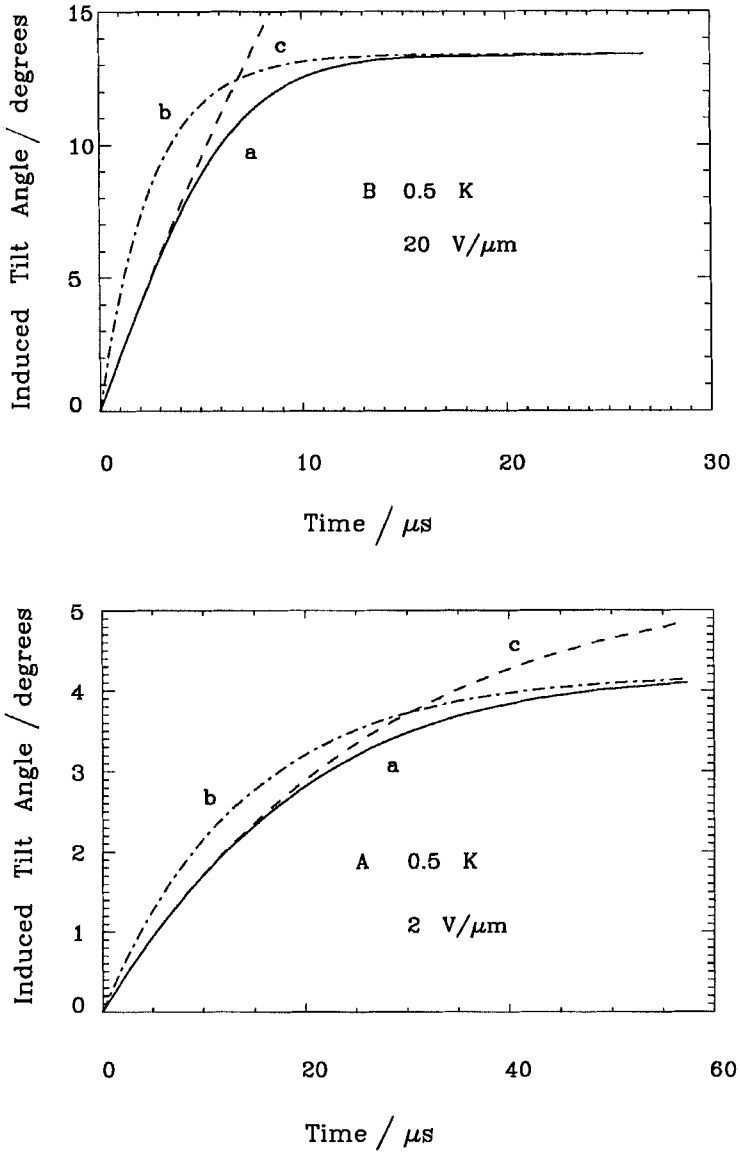

Figure 4. (A) Temporal evolution of the induced tilt angle for the case of the small electric field and close to the S_A^*–S_C^* transition: (a) the exact solution calculated from equation (9); (b) the approximate solution calculated from equation (15); and (c) the linear approximation calculated from equation (11). (B) Similar to (A) with higher electric field.

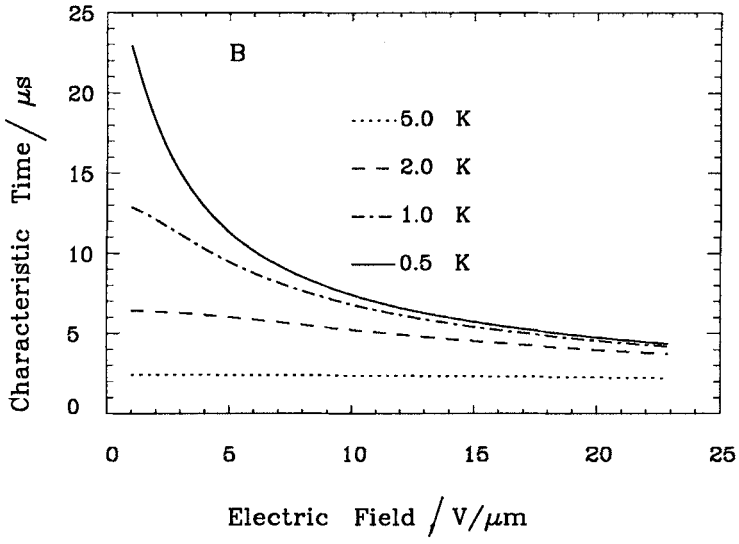

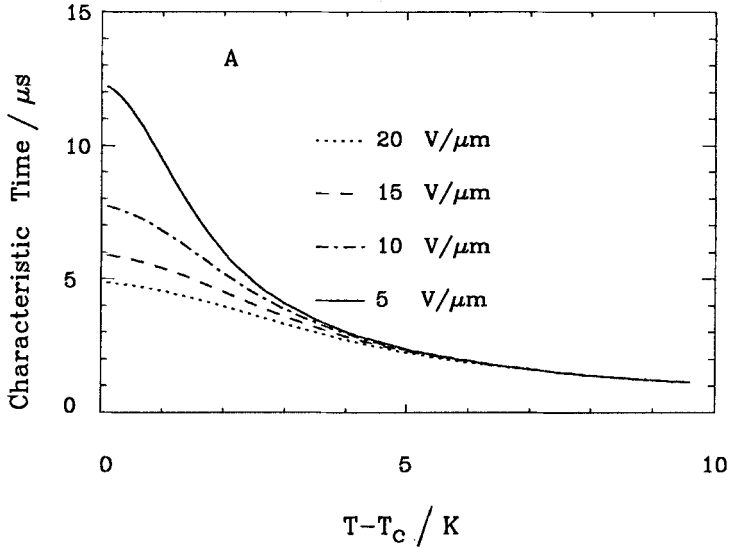

Figure 5. (A) Characteristic time for the rise of the induced tilt angle versus temperature for different field strengths. (B) Characteristic time for the rise of the induced tilt angle versus applied electric field strength at different temperatures.

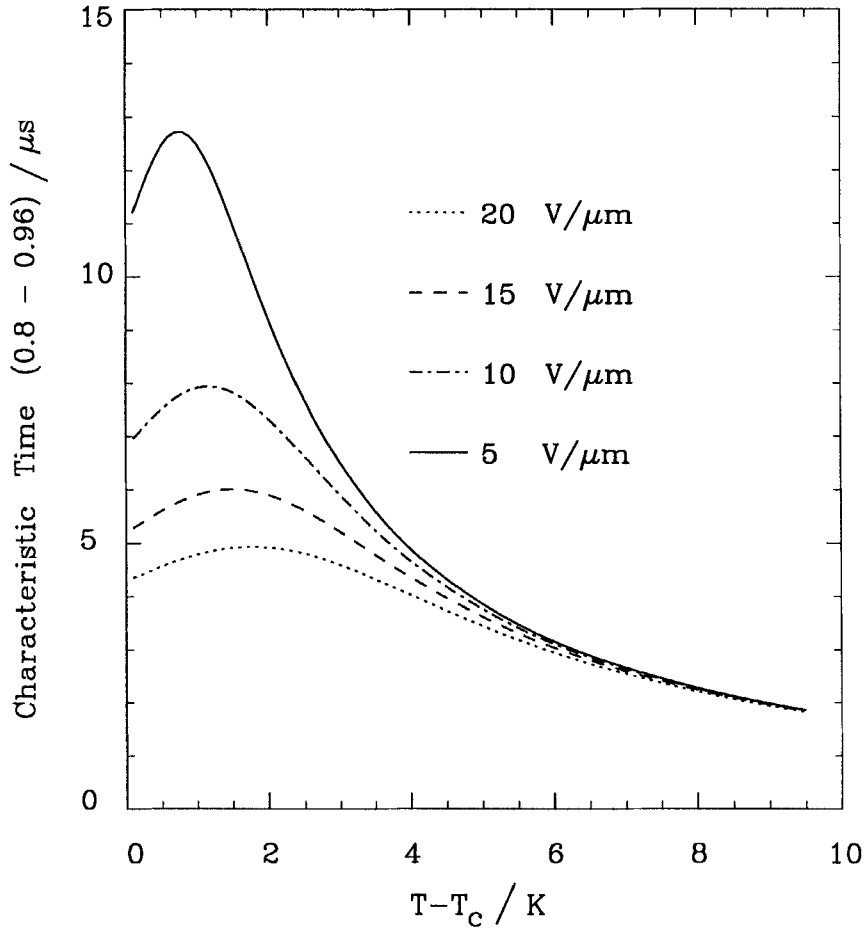

Figure 6. Characteristic time for the rise of the induced tilt angle from 0·8 to 0·96 of its steady state value versus temperature for different field strengths.

small tilt angles. This has not been observed because the measured characteristic time is determined from the early stages of the switching.

The decrease of the characteristic time near the transition results from the dominance of the non-linear term over the linear one. Consider the integrand in equation (3) as a potential energy for two coupled oscillators, one linear and the other non-linear. The non-linear oscillator will cause the response to be faster as the temperature decreases because θ, and hence the energy, is larger. The linear term will cause the slowing down because it becomes soft ($a \rightarrow 0$) as $T \rightarrow T_c$. As a result, at a certain temperature the non-linear term dominates and a maximum is observed, as shown in figure 6. When measuring the optical response time, the maximum may be observed. However, its height is small and might fall within the experimental error. Careful measurement should verify these predictions. Such a measurement will provide important information on the type of the transition since the term 'critical slowing down' is a fundamental concept from the theory of critical phenomena. The existence of the critical slowing down implies the existence of critical exponents for the relaxation time, and for corresponding observables of the system [19].

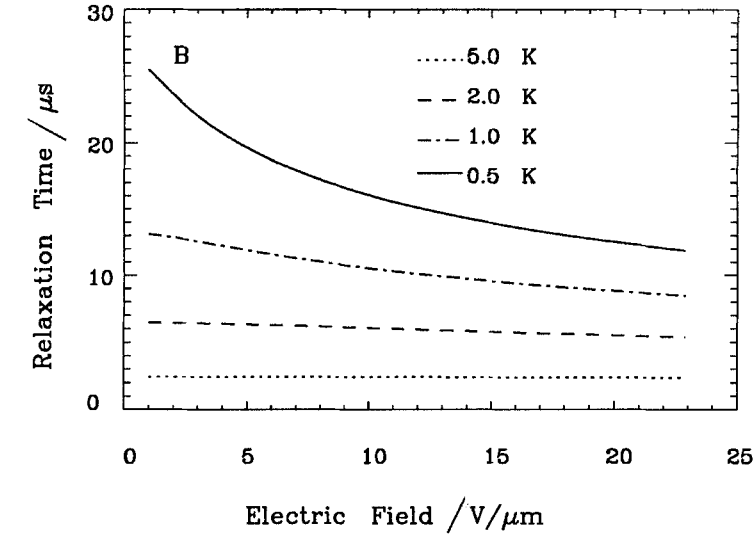

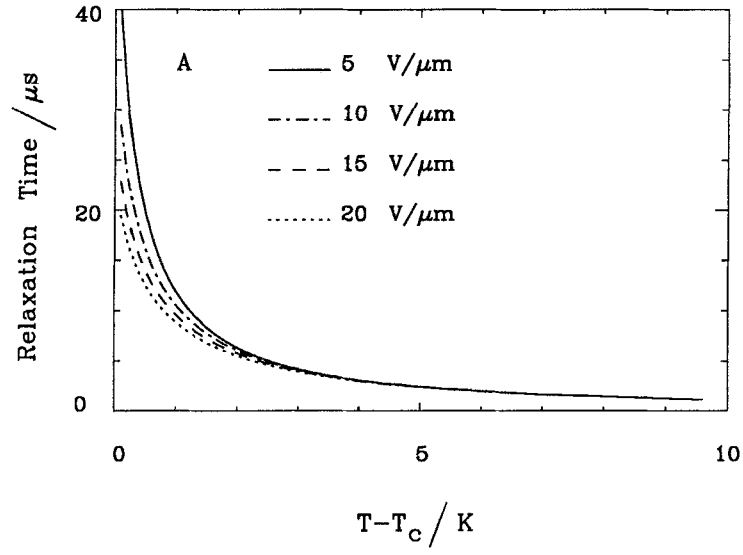

Figure 7. (A) Relaxation time after the field was switched OFF versus temperature at different field strengths. (B) Relaxation time after the field was switched OFF versus the field at different temperatures.

The finite value of the characteristic time at $T = T_c$ is a result of including the non-linear θ^3 term. According to the linear approximation the characteristic time diverges, a result which has never been observed experimentally. From equation (9) one can find the time interval τ_ε at $T = T_c$ required for θ to change from $\theta = 0$ to any fraction ε of the steady-state induced tilt angle θ_s, that is to $\theta = \varepsilon\theta_s$:

$$\tau_\varepsilon\Big|_{T=T_c} = \frac{\eta_\theta}{6b\theta_s^2}\left\{2\sqrt{3}\arctan\left(\frac{1+2\varepsilon}{\sqrt{3}}\right) - \ln\left(\frac{(1-\varepsilon)^2}{1+\varepsilon+\varepsilon^2}\right) - \frac{\pi}{\sqrt{3}}\right\}. \tag{22}$$

This shows that the characteristic time is finite at $T = T_c$, and that it decreases with the field as $E^{-2/3}$ by substituting the expression for θ_s at $T = T_c$ from equation (14). As mentioned earlier, the $c\chi_p$ product may be determined by measuring the finite values for θ_s and $d\theta/dE$ at $T = T_c$. By also measuring the characteristic time at $T = T_c$, the viscosity η_θ at $T = T_c$ may be obtained. We observe that η_θ could not show the critical behaviour proposed by Gouda *et al.* [18] because such critical behaviour would require that the characteristic time diverges or that $c\chi_p$ exhibits critical behaviour. Since the induced tilt angle does not show a divergence experimentally at $T = T_c$, then according to equation (14), $c\chi_p$ does not diverge and therefore η_θ will not exhibit a critical behaviour near the S_A^*–S_C^* transition.

The relaxation time τ_{rel} calculated from equation (19) with $\nu = e = 2{\cdot}718$ as a function of temperature and field is shown in figure 7, respectively. The temperature dependence of τ_{rel} is such that it decreases with temperature and saturates far from T_c. It is enhanced near T_c much more than the characteristic response time shown in figure 5 (A). In this sense we say that the relaxation exhibits more critical slowing down than does the response. The value of τ_{rel} should drop to zero at $T = T_c$ although τ_0 diverges as $T \to T_c$. The field dependence of τ_{rel} is strong near the transition (figure 7 (B)) and it has no field dependence far from the transition, as expected from equation (19). Comparing figure 7 (B) to 5 (B), the field dependence of τ_{rel} is similar to that of the response time and the two characteristic times have approximately the same values. This suggests that the response to a monopolar square voltage pulse may look almost symmetric only far from the transition or where the linear approximation holds.

5. The electro-optic response

5.1. *General considerations*

Linearly polarized light propagating along $\hat{x}$ through the structure of figure 1, in general, will be decomposed inside the medium into two independent eigenwaves, the ordinary and extraordinary, with the refractive indices $n_o = \sqrt{\varepsilon_\perp}$ and $n_e = \sqrt{\varepsilon_\parallel}$, respectively. Here $\varepsilon_\perp$ and $\varepsilon_\parallel$ are the optical dielectric constants perpendicular and parallel, respectively, to the director. To produce maximum contrast ratio, an electroclinic device may be operated as follows: In the off state, the cell is rotated around the propagation direction such that only one of the two eigenwaves is excited and therefore the light leaves the cell without a change in its polarization state. When placed between crossed polarizers the device has zero transmission. With the application of an electric field, the two eigenmodes are excited. This causes the state of polarization of the emerging light to change in a way which depends on the cell thickness of the cell, producing a non-zero output.

The emerging light from the cell is, in general, elliptically polarized. The angle between the principal axis of the ellipse α and the direction of incident polarization is given by

$$\alpha = \Omega - \tfrac{1}{2}\arctan[\tan(2\Omega)\cos\delta]. \tag{23}$$

Here $\delta = k_0 d\Delta n$ is the phase lag between the two eigenwaves where $k_0 = 2\pi/\lambda_0$ is the wave vector of light in the external isotropic medium, and Ω is the angle between the incident polarization and the optic axis.

To form a half-wave plate $\delta = (2m+1)\pi$ with $m = 0, 1, 2, \ldots$. When this condition is satisfied, the output is linearly polarized with its plane of polarization rotated by an angle $\alpha = 2\Omega$. In the case of a surface stabilized ferroelectric liquid crystal, $\Omega = 2\theta$, and if $\theta \approx \pi/8$ then $\alpha \approx \pi/2$ and ideally 100 per cent transmission is obtained in the ON state. In the electroclinic case $\theta < \pi/8$ for currently available mixtures, and therefore the ON state is less bright. One can enhance the ON state by applying a bipolar voltage such that $\Omega = 2(\theta_+ + \theta_-)$ where θ_+ and θ_- are the induced tilts for the positive and negative voltages, respectively.

To describe the electroclinic electro-optic response, it is sufficient to calculate the response to a step potential such that the field changes very quickly from 0 to E, where the RC time constant is very small compared to the optical switching response time. However, some electroclinic materials exhibit an optical response time on the order of 100 ns, so that the RC time constant becomes important. For all presently available mixtures which exhibit such a fast switching, the electroclinic effect is low and the induced tilt angle is a fraction of one degree or at most a few degrees. Therefore for these high-speed electroclinics, the linear approximation is adequate for most purposes. The growth of the applied field may be approximated as an exponential

$$E(t) = E[1 - \exp(-t/RC)], \tag{24}$$

where R and C are the electroclinic equivalent resistance and capacitance, respectively. The linear approximation solution to the dynamic equation given in equation (11), without the θ^3 term, becomes

$$\theta(t) = \frac{\theta_0}{\tau_0 - RC}\{\tau_0[1 - \exp(-t/\tau_0)] - RC[1 - \exp(-t/RC)]\}, \tag{25}$$

where θ_0 and τ_0 are given in equations (12) and (13). The first term grows with time constant τ_0 while the second term grows with RC. When RC is comparable to τ_0, its effect becomes important. If $\tau_0 \ll RC$ then the response is limited by the RC time constant. Equation (25) assumes that the capacitance does not change with time due to a growth of the polarization, described in equation (2). Since we consider here the case of small induced tilt angles, the polarization is very small compared to its value in the S_C^* phase. For induced tilt angles of a few degrees and the standard values of $c\chi_p$ we find that the polarization capacitance is smaller than the geometric capacitance by a factor of 10 to 15. Therefore the polarization capacitance may be neglected compared to the geometric capacitance, and the change of C with time is negligible. However, for certain electroclinic mixtures, where the polarization is very high, the change of C with time must be considered, and might produce some additional non-linearities in the switching behaviour.

5.2. *Reflection and transmission coefficients*

For incident light propagating along $\hat{x}$ and linearly polarized such that its polarization vector E_0 makes an angle Ω with the optic axis direction on the yz plane

(figure 8), the complex amplitudes of the ordinary and the extraordinary waves inside the structure are given by

$$\left.\begin{aligned}\mathbf{E}_o &= -E_0 \sin\Omega \exp(ik_0 n_o x)\hat{\mathbf{o}},\\ \mathbf{E}_e &= E_0 \cos\Omega \exp(ik_0 n_e x)\hat{\mathbf{e}}.\end{aligned}\right\} \tag{26}$$

Here $\hat{\mathbf{o}}$ and $\hat{\mathbf{e}}$ are unit vectors in the direction of the ordinary and extraordinary axes, respectively. For a more complete description we assume the two substrates have different refractive indices, n_{g1}, and n_{g2} and that multiple reflections take place. Since the two eigenwaves are orthogonal inside the medium, they cannot interfere and each of them is treated as an independent plane wave exhibiting multiple reflections from the two boundaries. The summation over all of these reflections (partial waves) yields the following expressions for the total transmitted and reflected amplitudes between crossed polarizers (see Appendix B)

$$E_t = 2E_0 \sin(2\Omega)\left\{\frac{n_{g1}n_e \exp(-ik_0 dn_e)}{(n_e+n_{g1})(n_e-n_{g2})-(n_e-n_{g1})(n_e-n_{g2})\exp(-2ik_0 dn_e)} - \frac{n_{g1}n_o \exp(-ik_0 dn_o)}{(n_o+n_{g1})(n_o+n_{g2})-(n_o-n_{g1})(n_o-n_{g2})\exp(-2ik_0 dn_o)}\right\}. \tag{27}$$

$$E_r = \tfrac{1}{2}E_0 \sin(2\Omega)\left\{\frac{(n_e+n_{g2})(n_e-n_{g1})-(n_e+n_{g1})(n_e-n_{g2})\exp(-2ik_0 dn_e)}{(n_e+n_{g1})(n_e+n_{g2})-(n_e-n_{g1})(n_e-n_{g2})\exp(-2ik_0 dn_e)} - \frac{(n_o+n_{g2})(n_e-n_{g1})-(n_o+n_{g1})(n_o-n_{g2})\exp(-2ik_0 dn_o)}{(n_o+n_{g1})(n_o+n_{g2})-(n_o-n_{g1})(n_o-n_{g2})\exp(-2ik_0 dn_o)}\right\}. \tag{28}$$

The transmittance and reflectance are given by $|E_t/E_0|^2$ and $|E_r/E_0|^2$, respectively. Equations (27) and (28) are correct if we neglect the reflections from the substrate–air interface, that is the liquid crystal is between two semi-infinite isotropic substrates. To include these reflections in the calculation, a good approximation would be to multiply each of the above expressions by the corresponding transmission or reflection coefficients of each of the corresponding substrate–air interfaces.

For an electrically-addressed device, the two substrates are usually identical, such that $n_{g1}=n_{g2}=n_g$, and equation (27) becomes

$$E_t = 2E_0 \sin(2\Omega)\left\{\frac{n_g n_e \exp(-ik_0 dn_e)}{(n_e+n_g)^2-(n_e-n_g)^2\exp(-2ik_0 dn_e)} - \frac{n_g n_o \exp(-ik_0 dn_o)}{(n_o+n_g)^2-(n_o-n_g)^2\exp(-2ik_0 dn_o)}\right\}. \tag{29}$$

The expressions given here are valid also for surface stabilized ferroelectic liquid crystals and tilted structures if the appropriate expressions for n_o and n_e are used. We note a difference between equation (29) and the equivalent expression obtained by Xue *et al.* [20]. The denominators of their expression are given by $(n_{o,e}-n_g)^2+(n_{o,e}+n_g)^2\exp(-2ik_0 dn_{o,e})$. These expressions are correct when one neglects the multiple reflections. In that case $n_o \approx n_e \approx n_g$, which is the condition they considered in their calculations. Therefore their results should be correct to within 1 per cent despite the error in their expression.

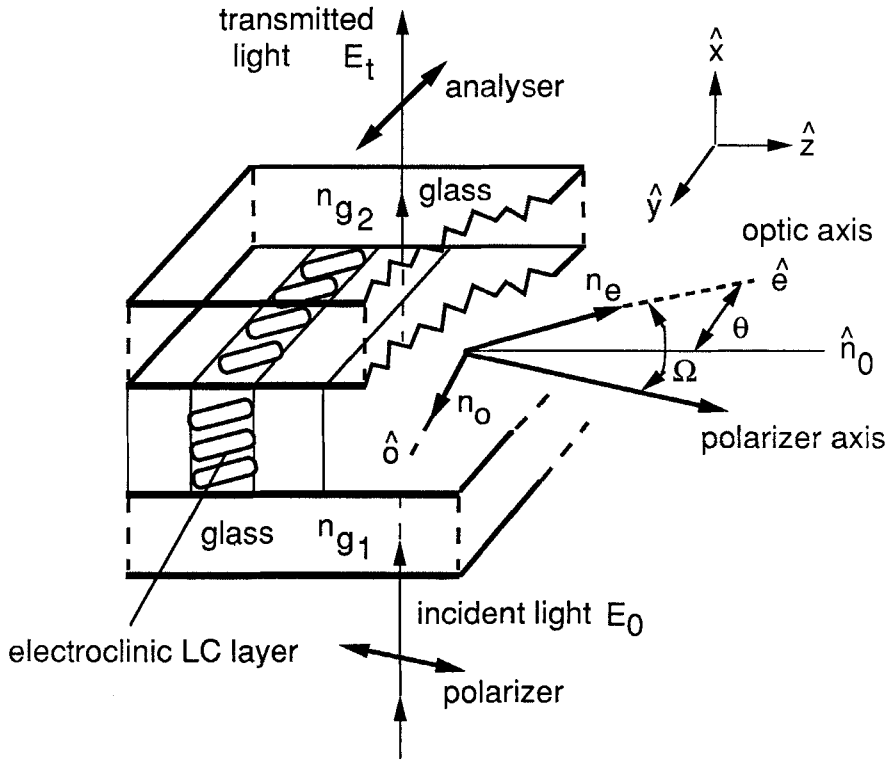

Figure 8. Geometry used for calculating the optical response of an electroclinic cell.

The commonly used simple formula for transmittance between crossed polarizers when multiple reflections are neglected is obtained from equation (29)

$$T_r = \sin^2(\tfrac{1}{2}k_0 d\Delta n)\sin^2(2\Omega), \tag{30}$$

where $\Delta n = n_e - n_o$ is the birefringence.

For a reflection-mode device, usually $n_{g1} \approx n_o \approx n_e$, and using equation (28) the reflectance through a polarized beamsplitter may be written as

$$R = \tfrac{1}{4}\sin^2(2\Omega)\{r_{eg_2}^2 + r_{og_2}^2 - 2r_{eg_2}r_{og_2}\cos(2k_0 d\Delta n)\}. \tag{31}$$

Here r_{og_2} and r_{eg_2} are the reflection coefficients of the ordinary and extraordinary waves from the second substrate, respectively (Appendix B).

If $n_{g2} > n_e$ then a simpler expression (equation (B 7)) may be obtained which is analogous to relation (30).

5.3. *Transmittance calculations*

To calculate the transmitted signal we use equation (27) with the constants: $n_{g1} = n_{g2} = 1{\cdot}5$, $n_o = 1{\cdot}55$, $n_e = 1{\cdot}67$ and $k_0 d = \pi/0{\cdot}12$ such that the cell acts as a half-wave plate. The transmittance versus the field at different temperatures is shown in figure 9 for the induced tilt angles of figure 2(A). Although the induced tilt is linear with the field for small angles and there is no threshold, the optical signal, which is determined by the geometry, grows as $\sin^2(2\theta)$. It deviates from linearity and appears to have a small threshold near zero field. The transmittance versus temperature at different field

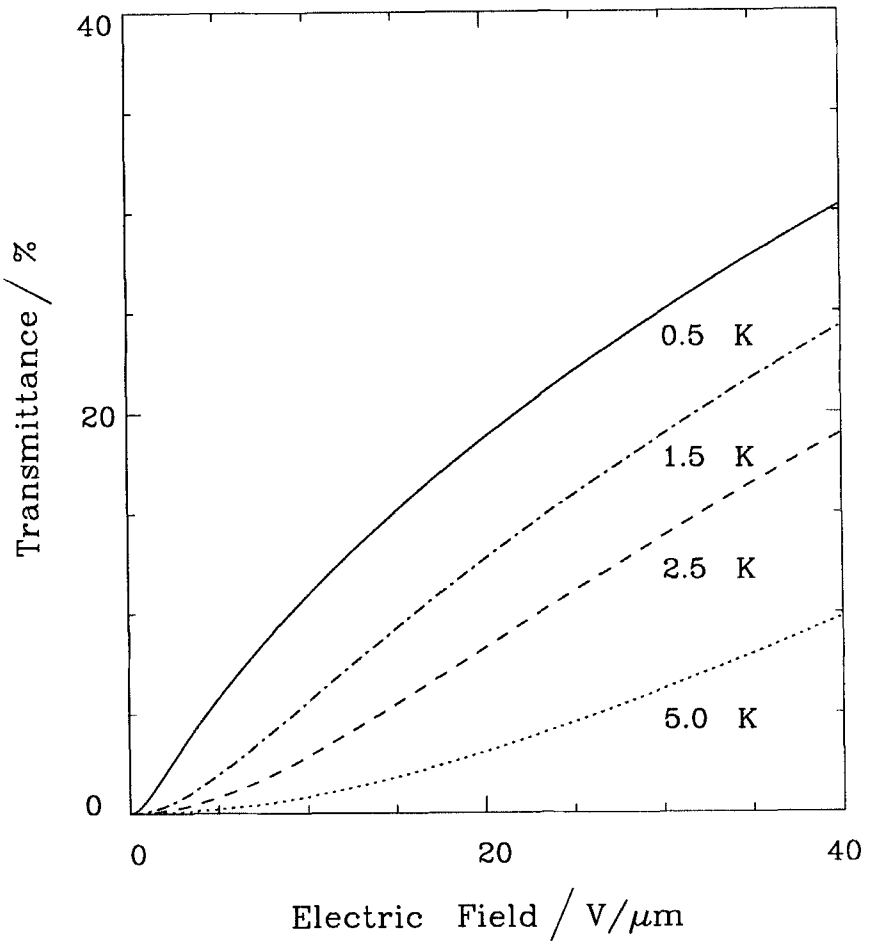

Figure 9. Transmittance through an electroclinic cell between crossed polarizers versus the field at different temperatures. The incident light is polarized along the optic axis at zero field such that the transmitted light is extinguished.

strengths exhibits similar behaviour to the induced tilt angle (figure 2(B)) versus temperature. The temporal evolution of the transmittance response to a step voltage at different fields and temperatures is shown in figure 10, corresponding to the evolution of the tilt angle in figure 3. Again, because the optical signal varies as $\sin^2(2\theta)$, there appears to be a small threshold. That is, the curves in figure 10 have a sigmoidal shape, rather than the linear behaviour in the beginning and saturation at the end which the induced tilt exhibits. For a surface stabilized ferroelectric liquid crystal cell the time until the signal reaches 10 per cent of its maximum (delay time) is larger by a factor of two than the rise time (10–90 per cent change in the transmittance) [20]. In the next section we will show that, in contrast to the surface stabilized ferroelectric liquid crystal case, the delay for an electroclinic is shorter than the rise time by a factor of approximately seven. In a temporal sense the electroclinic response is more analogue than the binary response of a surface stabilized ferroelectric liquid crystal. In addition, the surface stabilized ferroelectric liquid crystal exhibits bistability [20].

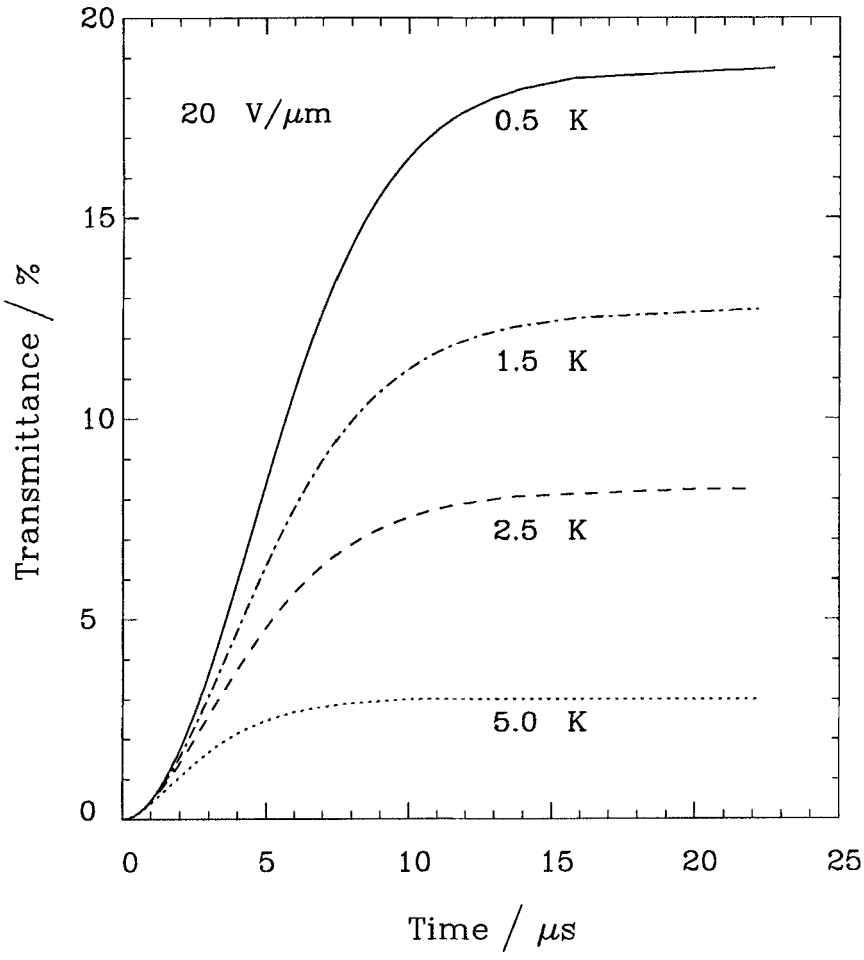

Figure 10. Temporal evolution of the transmittance for the geometry of figure 8 at constant field and different temperatures.

5.4. *Optical response time calculations*

Since the only time dependent term in the expression for the transmittance is $\sin^2(2\theta)$, one can derive an expression for the optical delay, rise and response times. The response time is the sum of the delay and rise times, which is the time required for the transmittance to change between 0 to 90 per cent. The 10 and 90 per cent change in the transmittance will be reached when $\theta=\theta_{0\cdot1}$ and $\theta=\theta_{0\cdot9}$ where

$$\left.\begin{aligned}\theta_{0\cdot1}&=0\cdot5\arcsin\left[0\cdot316\sin(2\theta_s)\right]\\ \theta_{0\cdot9}&=0\cdot5\arcsin\left[0\cdot948\sin(2\theta_s)\right].\end{aligned}\right\} \tag{32}$$

Substituting these expressions into equation (9) one obtains the following expression for the delay τ_d, response τ_{res}, and rise τ_{rise} times, respectively

$$\tau_d=\frac{\eta_\theta}{6b\theta_s^2+2a}\left(g(0)-g(\theta_{0\cdot1})\right), \tag{33}$$

$$\tau_{res}=\frac{\eta_\theta}{6b\theta_s^2+2a}(g(0)-g(\theta_{0\cdot9})), \tag{34}$$

$$\tau_{rise}=\frac{\eta_\theta}{6b\theta_s^2+2a}(g(\theta_{0\cdot1})-g(\theta_{0\cdot9})). \tag{35}$$

If one uses the exponential growth in either equation (11) or (15) then equations (33)–(35) become

$$\tau_d=\tau_\theta \ln\left(\frac{\theta_s}{\theta_s-\theta_{0\cdot1}}\right), \tag{36}$$

$$\tau_{res}=\tau_\theta \ln\left(\frac{\theta_s}{\theta_s-\theta_{0\cdot9}}\right), \tag{37}$$

$$\tau_{rise}=\tau_\theta \ln\left(\frac{\theta_s-\theta_{0\cdot1}}{\theta_s-\theta_{0\cdot9}}\right), \tag{38}$$

where τ_θ stands for τ_0 and τ_s in equations (13) and (16), respectively. Since $\theta_s<20°$, then $\theta_{0\cdot1}$ and $\theta_{0\cdot9}$ may be approximated as: $\theta_{0\cdot1}\approx0\cdot316\theta_s$ and $\theta_{0\cdot9}\approx0\cdot948\theta_s$, yielding

$$\left.\begin{aligned}\tau_d&\approx0\cdot379\tau_\theta,\\ \tau_{res}&\approx2\cdot956\tau_\theta,\\ \tau_{rise}&\approx2\cdot577\tau_\theta.\end{aligned}\right\} \tag{39}$$

Similar expressions could be found for the fall times using equations (18) and (19) when the fall is relaxation type, or equations (29) and (21) for the bipolar switching case.

In figures 11 and 12 we show the optical delay and rise times calculated from relations (33)–(35). The general behaviour as a function of field and temperature is similar to that of the characteristic time shown in figure 5. The optical characteristic times of equation (39) agree with the relationship of their values from figures 11 and 12 to the characteristic times (figure 5) in the linear regime. The critical slowing down is observed in the delay time versus temperature but not in the rise and response times. The optical rise (figure 11 (B)) time exhibits the maximum mentioned in § 2 (figure 6). Again, the maximum appears more pronounced for late stages of switching since it is higher in the rise time than in the response time. Figures 9–12 show that in general, optical response measurements can provide important information on the switching mechanism for the electroclinic effect. The figures may also be used for device applications in helping to determine optimal operation conditions.

6. Conclusions

We have investigated theoretically the switching behaviour and electro-optic response of the electroclinic effect in chiral smectic A liquid crystals. An exact analytic solution was found for the dynamic equation of the θ motion up to the θ^4 term in the Landau expansion of the free energy. The inclusion of this term is important in explaining certain properties near the transition, even for small angles, and it becomes essential for the case of induced tilt angles larger than a few degrees. Among the properties which the non-linear term adds are the following: (1) the characteristic time and the induced tilt have a finite value at $T=T_c$ and do not diverge; (2) the characteristic time has a strong field dependence near the transition; (3) the characteristic time exhibits a critical slowing down only in the early stages of the switching, while in later

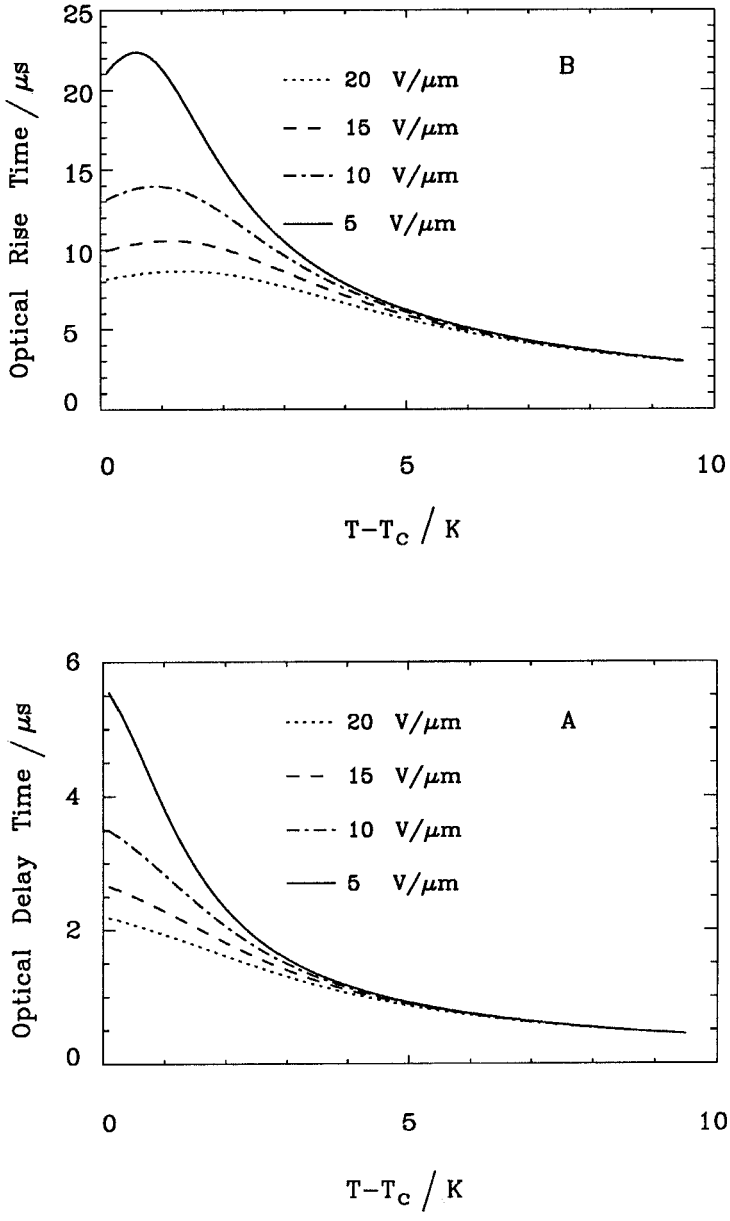

Figure 11. (A) The delay time of the optical response versus temperature for different field strengths. (B) Similar to (A) for the rise time of the optical response.

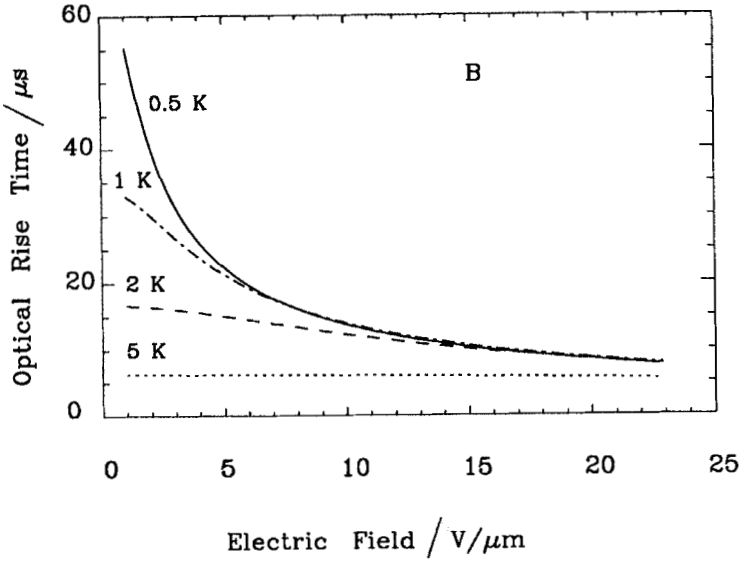

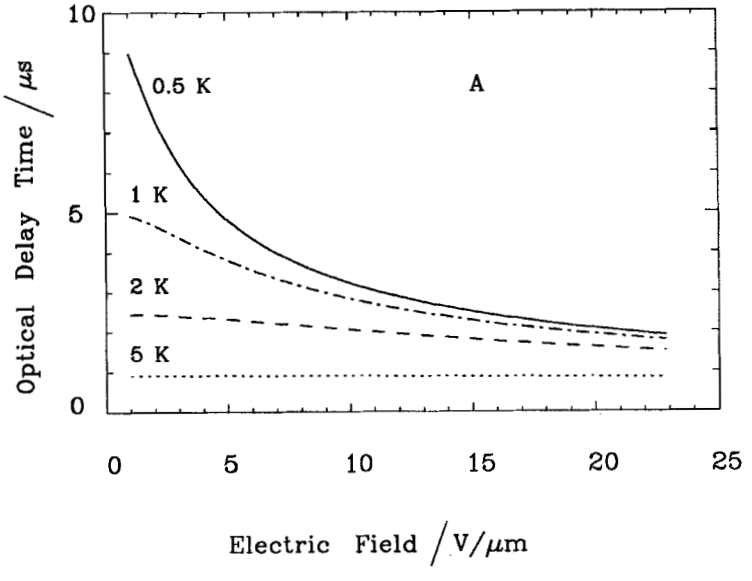

Figure 12. (A) The delay time for the optical response versus the applied electric field at different temperatures. (B) Same as (A) for the rise time of the optical signal.

stages it exhibits a maximum as a function of temperature close to the transition temperature and decreases below that towards a finite value at $T=T_c$; (4) the latter maximum shifts to higher temperatures and becomes less pronounced as the field increases; (5) the induced tilt asymptotes to $E^{1/3}$ for high fields at temperatures close to the transition; (6) the slope $d\theta/dE$ is enhanced near the transition but has a finite value at T_c; (7) the relaxation behaviour after the field was switched off depends on the previously applied field solely due to the non-linear term; and (8) as a result of (7) the electroclinic response to a monopolar square pulse voltage is not symmetric, however it might appear that way for cases where the linear approximation is valid. We suggest that the coupling constant $c\chi_p$ between the tilt and the field, as well as its field dependence, may be determined from measurements of the finite values of the induced tilt and characteristic time near T_c. These values will also determine directly the viscosity. We note that the viscosity cannot show a critical behaviour near the transition, contrary to a recent suggestion [18]. Experimental confirmation of the new results presented here will improve our understanding of the electroclinic effect and the S_A^*–S_C^* transition.

The electro-optic response of an electroclinic cell has been considered in detail. This response is a powerful technique for exploiting the switching behaviour of the electroclinic effect from both fundamental and practical viewpoints as a fast analog electro-optic device. A detailed experimental investigation of S_A^* liquid crystals and the development of similar theory for tilted and non-uniform structures will follow.

We are grateful to Professor N. Clark, A. Gabor, P. Barbier, and R. Rice for their comments on the manuscript. This work was performed under the National Science Foundation Engineering Research Center Grant No. CDR-862236.

Appendix A

Derivation of the analytic solutions in § 3

The three roots of the cubic equation (6) for $a>0$ are given by

$$\left.\begin{aligned}\theta_1&=U_+ + U_-,\\ \theta_2&=-\tfrac{1}{2}[\theta_1+\mathrm{i}\sqrt{3}(U_+-U_-)],\\ \theta_3&=\theta_2^*.\end{aligned}\right\} \tag{A 1}$$

Since $U_\pm$ are always real the only real solution is $\theta_1=\theta_s$, as given in equation (7). By factoring out $(\theta-\theta_s)$ we find

$$c\chi_p E-a\theta-b\theta^3=(\theta-\theta_s)(\theta^2+\theta\theta_s+\theta_s^2-3U_+U_-) \tag{A 2}$$

and the integration of the dynamic equation (4) is straightforward. To distinguish between the different cases of step field (equation (9)), relaxation (equation (19)) and bipolar pulse field (equation (20)), different initial conditions must be taken. For the general description we let the field switch from 0 at $t=0$ to E_1 very quickly and then switch very quickly to the level E_2 at the time t_1. The solution during the interval $0<t<t_1$, is given by

$$t=\frac{\eta_\theta g(0)-g(\theta,\theta_{s1},E_1)}{6b[(\theta_{s1}^2+(a/3b)]}. \tag{A 3}$$

The solution for $t>t_1$ is obtained by taking the initial condition $\theta=\theta_{s1}$ at $t=t_1$ and $\theta=\theta_{s2}$ as $t\to\infty$ and is given by

$$\frac{6b}{\eta_\theta}\left(\theta_{s2}^2+\frac{a}{3b}\right)t=g[\theta(t_1),\theta_{s1},E_1]-g(\theta,\theta_{s2},E_2)+\frac{6b}{\eta_\theta}\left(\theta_{s1}^2+\frac{a}{3b}\right)t_1. \tag{A 4}$$

Equation (9) is obtained from equation (A 3) by noting that $\theta_s=\theta_{s1}$ and $E=E_1$. Equation (18) is obtained by direct integration of the dynamic equation (4) with $E=0$ and the initial condition $\theta=\theta_s$ at $t=0$ where t is measured from the moment the field is switched off. Equation (20) is obtained from equation (A 4) by substituting $\theta_{s1}=\theta_{s+}$, $E_+=E_1$, $\theta_{s2}=\theta_{s-}$, $E_-=E_2$ and $t_1=t_+$. The case of $\zeta\ll1$ is achieved by a Taylor series expansion of $U_\pm$ in equation (8) up to the first order, yielding

$$\left.\begin{aligned}U_+&\approx\left(\frac{c\chi_pE}{b}\right)^{1/3}\left(1+\frac{\zeta}{6}\right),\\ U_-&\approx\left(\frac{c\chi_pE}{b}\right)^{1/3}\left(-\frac{\zeta}{6}\right),\end{aligned}\right\} \tag{A 5}$$

which directly gives equation (14). The case of $\zeta\gg1$ is treated by writing $U_\pm$ in the form

$$U_\pm=\left(\frac{c\chi_pE}{2b}\sqrt{\zeta}\right)^{1/3}\left(\frac{1}{\sqrt{\zeta}}\sqrt{\left(1+\frac{1}{\zeta}\right)}\right)^{1/3}. \tag{A 6}$$

Again a Taylor series expansion to the first order yields

$$U_\pm=\pm\sqrt{\left(\frac{a}{3b}\right)}+\frac{c\chi_pE}{2a}, \tag{A 7}$$

which directly results in the linear approximation of equation (12).

In order to derive the exponential growth in equation (15) we write equation (9) in the form

$$\theta(t)=\theta_s-\exp\left(\frac{g(0)+h(\theta)}{2}\right)\exp\left(\frac{-t}{\tau_s}\right), \tag{A 8}$$

where $h(\theta)=2\ln(\theta_s-\theta)-g(\theta)$.

We assume that $h(\theta)$ does not change significantly over the range from $\theta=0$ to $\theta=\theta_s$ and therefore we may replace it with its value at $\theta=0$ and directly obtain relation (15). This approximation is therefore justified when θ_s is small, as was shown in figure 4. Therefore equation (15) may replace equation (11) because it covers the same range of induced tilt angles, and also gives the correct expressions for the steady-state induced tilt and the characteristic time.

To see how one obtains $\tau_s\approx\tau_0$ in the limit $\zeta\gg1$ (small θ_s), we use the result in equation (A 7) and write

$$U_\pm\approx\pm\sqrt{\left(\frac{a}{3b}\right)}. \tag{A 9}$$

Substituting these in equation (16) directly shows that $\tau_s\approx\tau_0$. For the limit $\zeta\ll1$ we substitute $U_\pm$ from equation (A 3) into equation (16) yielding the $E^{-2/3}$ behaviour of τ_s in equation (17).

Appendix B

Derivation of the transmittance and reflectance coefficients

The summation over all of the partial waves resulting from the reflections from the liquid crystal substrate interfaces is a simple geometric series. Performing these summations for both the ordinary and extraordinary waves yields the following expressions for the amplitudes of the two waves at the boundary $x=d^+$

$$\left.\begin{aligned}\mathbf{E}_{od^+} &= -E_0 \sin\Omega\left(\frac{t_{g_1o}t_{og_2}\exp(-ik_0dn_o)}{1+r_{g_1o}r_{og_2}\exp(-2ik_0dn_o)}\right)\hat{\mathbf{o}}\\ \mathbf{E}_{ed^+} &= E_0 \cos\Omega\left(\frac{t_{g_1e}t_{eg_2}\exp(-ik_0dn_e)}{1+r_{g_1e}r_{eg_2}\exp(-2ik_0dn_e)}\right)\hat{\mathbf{e}}\end{aligned}\right\} \tag{B 1}$$

and similarly for the amplitudes at $x=0^-$

$$\left.\begin{aligned}\mathbf{E}_{o0^-} &= -E_0 \sin\Omega\left(\frac{r_{g_1o}+r_{og_2}\exp(-2ik_0dn_o)}{1+r_{g_1o}r_{og_2}\exp(-2ik_0dn_o)}\right)\hat{\mathbf{o}},\\ \mathbf{E}_{e0^-} &= E_0 \cos\Omega\left(\frac{r_{g_1e}r_{eg_2}\exp(-2ik_0dn_e)}{1+r_{g_1e}r_{eg_2}\exp(-2ik_0dn_e)}\right)\hat{\mathbf{e}}.\end{aligned}\right\} \tag{B 2}$$

Here $\hat{\mathbf{o}}$ and $\hat{\mathbf{e}}$ designate the directions of the ordinary and the extraordinary axes, respectively. The coefficients t_{g_1o}, t_{og_2}, t_{g_1e}, t_{eg_2}, r_{g_1o}, r_{og_2}, r_{g_1e}, r_{eg_2} are the Fresnel transmission and reflection coefficients of the **o** and **e** waves from the two boundaries and are given by

$$\left.\begin{aligned} t_{g_1o} &= \frac{2n_{g1}}{n_o+n_{g1}}; & r_{g_1o} &= \frac{n_o-n_{g1}}{n_o+n_{g1}},\\ t_{og_2} &= \frac{2n_o}{n_o+n_{g2}}; & r_{og_2} &= \frac{n_{g2}-n_o}{n_{g2}+n_o},\\ t_{g_1e} &= \frac{2n_{g1}}{n_e+n_{g1}}; & r_{g_1e} &= \frac{n_e-n_{g1}}{n_e+n_{g1}},\\ t_{eg_2} &= \frac{2n_e}{n_e+n_{g2}}; & r_{eg_2} &= \frac{n_{g2}-n_e}{n_{g2}+n_e}.\end{aligned}\right\} \tag{B 3}$$

The total field amplitudes at the two boundaries are

$$\left.\begin{aligned}\mathbf{E}_{td^+} &= \mathbf{E}_{od^+}+\mathbf{E}_{ed^+},\\ \mathbf{E}_{t0^-} &= \mathbf{E}_{o0^-}+\mathbf{E}_{e0^-}.\end{aligned}\right\} \tag{B 4}$$

If the analyser is crossed with respect to the polarizer, then its axis is represented by the unit vector

$$\hat{\mathbf{A}} = \sin\Omega\hat{\mathbf{e}} + \cos\Omega\hat{\mathbf{o}} \tag{B 5}$$

and the transmitted and reflected amplitudes are given by

$$\left.\begin{aligned}E_t &= \mathbf{E}_{td^+}\cdot\hat{\mathbf{A}},\\ E_r &= \mathbf{E}_{t0^-}\cdot\hat{\mathbf{A}}.\end{aligned}\right\} \tag{B 6}$$

Equation (B 3) is substituted into equations (B 1) and (B 2). The result is substituted in equation (B 4) which, when combined with equation (B 5) in equation (B 6), directly

yields equations (27) and (28). In this formulation one finds expressions for E_t and E_r with any orientation of the analyser by including the appropriate expression for $\hat{\mathbf{A}}$.

To obtain equation (31), we take $n_{g1} \approx n_o \approx n_e$ for a reflection-mode device in relation (28). If $n_{g2} > n_e$ then we can approximate $r_{eg_2} \approx r_{og_2} \approx r_2$ with the result that

$$R = R_2 \sin^2 (k_0 d \Delta n) \sin^2 2\Omega, \tag{B 7}$$

for $R_2 = |r_2|^2$ taken as the average between $|r_{og_2}|^2$ and $|r_{eg_2}|^2$. Equation (B 7) is analogous to equation (30) used for transmission-mode device. Note that the phase in equation (B 7) is double that in equation (30) because the beam travels back and forth through the liquid crystal.

References

[1] GAROFF, S., and MEYER, R. B., 1977, *Phys. Rev. Lett.*, **38,** 848.
[2] GAROFF, S., and MEYER, R. B., 1979, *Phys. Rev.* A, **19,** 338.
[3] POZHIDAYEV, E. P., BLINOV, L. M., BERESNEV, L. A., and BELYAYEV, V. V., 1985, *Molec. Crystals liq. Crystals*, **124,** 359.
[4] BERESNEV, L. A., BLINOV, L. M., OSIPOV, M. A., and PIKIN, S. A., 1988, *Molec. Crystals liq. Crystals* A, **158,** 3.
[5] QIU, R., HO, J. T., and HARK, S. K., 1988, *Phys. Rev.* A, **38,** 1653.
[6] LI, Z., and ROSENBLATT, C., 1989, *Phys. Rev.* A, **39,** 1594.
[7] BAHR, CH., and HEPPKE, G., 1987, *Liq. Crystals*, **2,** 825.
[8] BAHR, CH., and HEPPKE, G., 1988, *Phys. Rev.* A, **37,** 3179.
[9] LI, Z., PETSCHEK, R. G., and ROSENBLATT, C., 1989, *Phys. Rev. Lett.*, **62,** 796; 1989, *Ibid.*, **62,** 1577(E).
[10] ANDERSON, G., DAHL, I., KELLER, P., KUCZYNSKI, W., LAGERWALL, S. T., SKARP, K., and STEBLER, B., 1987, *Appl. Phys. Lett.*, **51,** 640.
[11] ABDULHALIM, I., MODDEL, G., and JOHNSON, K. M., 1989, *Appl. Phys. Lett.*, **55,** 1603.
[12] ANDERSON, G., DAHL, I., KUCZYNSKI, W., LAGERWALL, S. T., SKARP, K., and STEBLER, B., 1988, *Ferroelectrics*, **84,** 285.
[13] OZAKI, M., HATAI, T., and YOSHINO, K., 1988, *Jap. J. appl. Phys.*, **27,** L1996.
[14] ABDULHALIM, I., and BENGUIGUI, L., 1990, *Phys. Rev.* A, **42,** 2114.
[15] NISHIYAMA, S., OUCHI, Y., TAKEZOE, H., and FUKUDA, A., 1987, *Jap. J. appl. Phys.*, **26,** L1787.
[16] LEE, S. D., and PATEL, J. S., 1989, *Appl. Phys. Lett.*, **54,** 1653; 1989, *Ibid.*, **55,** 122.
[17] XUE, J., and CLARK, N. A., 1990, *Phys. Rev. Lett.*, **64,** 307.
[18] GOUDA, F., SKARP, K., ANDERSSON, G., KRESSE, H., and LAGERWALL, S. T., 1989, *Jap. J. appl. Phys.*, **28,** 1887.
[19] See for example: VERBEUNE, A., 1989, *Instabilities and Nonequilibrium Structures*, Vol. II, *Dynamical Systems and Instabilities*, edited by E. Tirapegui and D. Villarroel (Kluwer Academic Publishers), pp. 131–143.
[20] XUE, J., HANDSCHY, M. A., and CLARK, N. A., 1987, *Ferroelectrics*, **73,** 305; 1987, *Liq. Crystals*, **2,** 707.